STRUCTURAL DESIGN AND MECHANICAL PERFORMANCE OF CORRUGATED STEEL WEB BOX GIRDERS IN CONTEMPORARY BRIDGE ENGINEERING

B. W. Gong
Abeer Abdullah Al Anazi
Nader Ghareeb
Ahmad Sedaghat

To evaluate the real-world performance of corrugated steel web box girders in modern bridges, this study investigates their structural design and mechanical behavior using a three-dimensional finite element modeling approach. The main girder scheme and corrugated steel web box girder configuration are defined, and two representative loading cases are considered: Case 1 with symmetric loading and Case 2 with eccentric loading. A prestressing system is incorporated and a spatial finite element model is established to assess key performance indicators, including ultimate flexural capacity, shear buckling behavior, and shear-stress resistance of the corrugated steel web. Results show that the vehicle-load eccentricity amplification factor is essentially unchanged (M2/M1 = 1.002), indicating near-identical responses between the two loading cases. With a positive-stress bias amplification factor of 1.20 and a shear-stress bias amplification factor of 1.51, the designed bridge demonstrates strong overall stability. Moreover, the computed shear stresses in the corrugated steel web remain below the allowable design limits, confirming that its mechanical behavior satisfies current bridge design standards. These findings support the practical adoption of corrugated steel web box girders and highlight their relevance for sustainable bridge construction.

Index Terms — corrugated steel web, bridge structure design, mechanical properties, sustainable development, spatial finite element modelling

https://doi.org/10.66033/judsc2024-103

INTRODUCTION

The newly developed corrugated steel web composite box girder bridge with a steel bottom plate enables the complementary advantages of steel and concrete to be fully utilized. This structural configuration enhances the overall stress performance of the girder while effectively mitigating common problems associated with concrete bottom slabs, such as cracking. By replacing the conventional concrete bottom plate with a steel one, the self-weight of the box girder can be substantially reduced, thereby improving its spanning capacity, simplifying on-site transportation and installation, and extending the service life of the bridge [1, 2, 3].

Corrugated steel web box girders represent a hybrid structural system in which the traditional concrete web is replaced by a corrugated steel web. This change in material and geometry is accompanied by a significant reduction in web thickness. However, compared with concrete webs, corrugated steel webs provide weaker support to the deck slab. As a result, the restraint conditions of the deck slab and the distortion and torsional behavior of the closed box-girder frame differ from those of conventional concrete box girders. Consequently, the transverse internal force distribution in the deck slab of corrugated steel web box girders also differs from that of traditional concrete box girders [4, 5, 6].

In recent years, the growing demand for transportation and logistics has led to increasing widths of highway and urban bridges. As a result, wide single-box multi-cell corrugated steel web prestressed concrete (PC) composite box girder bridges have been increasingly adopted in practice [7, 8]. To date, more than 30 corrugated steel web PC composite box girder bridges with more than two cells have been constructed in China. Statistical analyses of completed and ongoing projects indicate that when the span exceeds 50 m, variable-depth structural forms combined with segmental cantilever construction methods are generally preferred from both economic and technical perspectives [9, 10, 11]. Accordingly, investigating the spatial mechanical behavior of variable-depth single-box multi-cell corrugated steel web PC box girder bridges has become an important research focus [12].

At present, the design and analysis of corrugated steel web PC composite box girder bridges commonly rely on methods such as the spatial truss model, the seven-degree-of-freedom thin-walled box girder model, planar beam lattice models, solid finite element models, and spatial grid models. However, the spatial truss model lacks sufficient refinement in capturing three-dimensional effects and cannot accurately describe phenomena such as shear lag, constrained torsion, and distortion [13, 14]. The seven-degree-of-freedom single-girder model incorporates warping bimoments on the basis of the conventional six-degree-of-freedom spatial truss model, allowing for the analysis of statically indeterminate shear flow distributions in thin-walled box sections. Although its computational cost is only slightly higher than that of the traditional model, it still fails to provide a refined representation of spatial effects such as shear lag and distortion [15, 16].

Planar beam lattice models can capture the nonuniform distribution of normal stresses across the cross-section, but they are unable to accurately simulate the combined effects of shear and torsion or the precise shear flow distribution in the top and bottom slabs. Furthermore, they neglect the out-of-plane behavior of local slab elements. Solid finite element models, on the other hand, can accurately represent the spatial mechanical response of bridge structures. However, their results are difficult to integrate with construction stage analysis, shrinkage and creep effects, and live load simulations typically required in design. Moreover, these models provide global stress responses that are not directly compatible with current reinforcement design specifications, making targeted reinforcement design challenging [17, 18, 19]. The post-processing of internal forces from solid elements is also complex and computationally demanding, which restricts their widespread application in routine design and limits their use mainly to localized analyses.

The spatial grid model discretizes a complex bridge structure into multiple plate components, each represented by an orthogonal beam lattice. In this approach, the stiffness of intersecting longitudinal and transverse

beams (six-degree-of-freedom beam elements) is used to approximate plate stiffness. Each plate is thus represented as a "mesh" of beam elements, and a structure composed of multiple plates can be modeled as a set of such meshes. Although this method is theoretically capable of simulating complex bridge forms—such as variable-depth single-box multi-cell corrugated steel web PC composite box girders—the modeling process is cumbersome and difficult to implement in practical engineering design [20, 21, 22].

The present study focuses on a large-span partially cable-stayed bridge, a structural type for which relatively few engineering examples and limited research are currently available. By deriving mechanical performance verification formulas and establishing detailed spatial finite element models, this work aims to provide methodological guidance for the structural design of corrugated steel web box girders in modern bridges. Considering the characteristics of both the main girder and the corrugated steel web, two loading scenarios are examined: symmetric vehicular loading (working condition 1) and eccentric vehicular loading (working condition 2). Corresponding prestressing schemes and spatial finite element models are developed. A mega-span partially cable-stayed bridge is selected as the case study, and the proposed models are used to investigate the mechanical performance of corrugated steel web box girders in three key aspects: flexural ultimate bearing capacity, shear buckling behavior, and shear stress resistance.

STRUCTURAL DESIGN AND MECHANICAL PROPERTIES OF CORRUGATED STEEL WEB BOX GIRDERS

Structural design of corrugated steel web box girders

Main girder configuration

Based on structural calculations and experience from comparable projects, the height of the girder at the middle pier is set to 5.5 m, while the height at the side pier and within the span is 2.6 m. The girder height varies according to two parabolic profiles, resulting in height-to-span ratios of 1/16.44 and 1/33.21. The main girder is constructed using a symmetrical cantilever method. The segment prior to closure is designated as the No. 0 segment and has a length of 10.37 m, while each single cantilever cast-in-place segment measures 4.72 m. Following engineering precedents, the closure segment lengths for both the side span and the mid-span are set at 3.11 m, and the cast-in-place section at the side-span support is 8.18 m long.

The main girder is made of C55 concrete. The top slab has a total width of 12.66 m, with wing slabs of 2.842 m each, and a box chamber width of 5.0 m. A unidirectional transverse slope of 1.82% is applied. The underside of the top slab is folded, and the slab thickness at the centerline of the box chamber is 0.27 m, gradually increasing toward the web-root region. The bottom slab thickness is 0.6 m at mid-span and increases to 1.0 m at the middle pier, following a cubic parabolic profile.

Because the corrugated steel webs replace conventional concrete webs, the torsional and distortion stiffness of the box girder is reduced. To compensate for this, one transverse diaphragm is installed in each side span and three are installed in the middle span. The diaphragm thickness is 0.80 m at steering positions and 0.60 m elsewhere. In addition, the corrugated steel webs near the top of the piers are lined internally with concrete in Sections 1 and 2, while the inner face of the corrugated web in Section 6 of the transition pier is also lined with concrete to enhance stiffness and durability.

Corrugated steel webs

The corrugated steel webs are fabricated using a 1900-type corrugation pattern, following the specifications for corrugated steel web composite bridges. The horizontal and diagonal flat lengths are 0.46 m, the diagonal projection is 0.44 m, and the corrugation height is 0.27 m. The bending radius depends on the web thickness. The web thickness varies from 16 mm to 25 mm near the middle pier, with four distinct thickness zones determined through structural analysis.

The steel grade selected is Q345D, and the webs are factory-fabricated in single units, which are subsequently welded together on site [23, 24]. Temporary bolting is used to control the joint gap (not exceeding 0.8 mm), followed by fillet welding to ensure continuity [25, 26]. The top slab is connected to the steel web through T-PBL shear connectors, while the bottom slab uses embedded shear keys with an embedment depth of 500 mm. The embedded portion of the web contains double rows of circular openings spaced at 150 mm, each with a diameter of 40 mm. Reinforcing bars of 30 mm diameter pass through these holes, and the upper and lower rows are staggered by 36 mm. A 25 mm diameter steel bar is welded along the bottom edge of the web. The connection between the corrugated web and the diaphragms is achieved using penetrated reinforcing bars in the transverse direction and bolts in the longitudinal direction.

Prestressing system

The prestressing system of the main girder combines internal and external tendons. Internal tendons are used in the top slab during cantilever construction and in both top and bottom slabs during closure. Tendon types 15-15 and 15-19 are adopted, with round anchorage systems. The characteristic tensile strength is $f_{pk} = 1830$ MPa, and the design control stress at anchorage is $0.75 f_{pk} = 1372.5$ MPa. Plastic ducts and vacuum grouting are employed for bonded tendons.

For external prestressing, 15-22 epoxy-coated unbonded strands are used, with a design control stress of $0.6 f_{pk} = 1098$ MPa. The dead weight and construction-stage loads are mainly resisted by the internal tendons, while the bridge deck pavement, parapets, and traffic loads are primarily carried by the external tendons. To facilitate inspection, maintenance, and replacement, the external tendons are designed for multiple tensioning cycles and enhanced corrosion protection.

Spatial finite element modeling

Geometric configuration A simply supported corrugated steel web composite box girder with a span of 40.32 m is selected as the prototype. Key parameters such as girder height, web inclination, material type, web thickness, and diaphragm spacing are varied for comparative modal analyses under different conditions. Figure 1 shows the typical cross section when the web inclination angle is zero, and Figure 2 illustrates the corrugation geometry.

Loading conditions Two loading scenarios are considered: symmetric and eccentric vehicle loading. These loading arrangements follow relevant code provisions. For the symmetric case (Figure 3), two lanes are loaded symmetrically with a combination of uniform load q and concentrated load p. The wheel loads are positioned such that their centerlines are located 160 cm from the pavement edge.

For the eccentric case (Figure 4), the lane loads are applied asymmetrically. The distances from the pavement

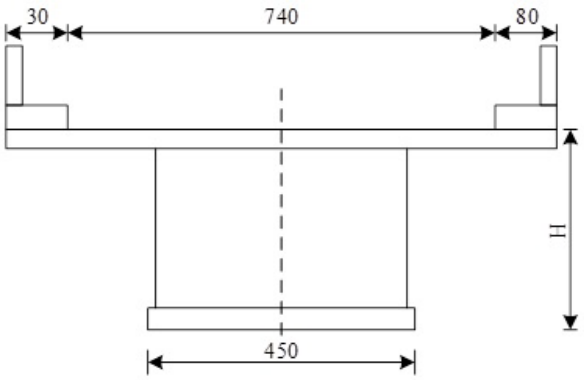

Figure 1: Typical cross section

Figure 2:

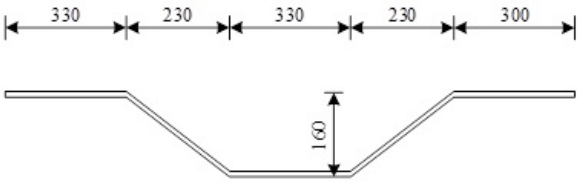

Figure 3: Corrugated size of steel web

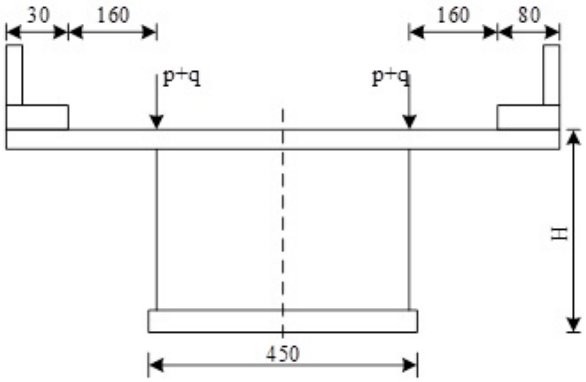

Figure 4: Working condition one

edge are 170 cm and 450 cm, respectively. From the static analyses, mid-span deflections, normal stresses in the slab, and shear stresses near the supports are extracted for comparison.

Modeling assumptions The following assumptions are adopted:

- Full composite action between the corrugated steel web and the concrete slabs, with no slip or connector failure.
- Prestressing tendons are not explicitly modeled.

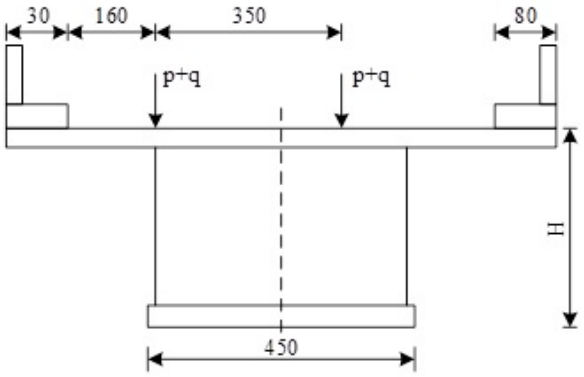

Figure 5: Working condition 2

- The corrugated web possesses sufficient flexural capacity, and flexural failure of the web is neglected.
- Material nonlinearities of steel and concrete are not considered.
- The effect of the pavement layer is ignored.

Material properties and boundary conditions The elastic modulus of concrete is $E_c = 3.09 \times 10^4$ MPa, with Poisson's ratio $\nu_c = 0.1155$ and unit weight $\rho_c = 28$ kN/m^3. The steel web has $E_s = 2.112 \times 10^5$ MPa, $\nu_s = 0.3128$, and $\rho_s = 73$ kN/m^3. The diaphragm properties match those of the concrete slabs. The design tensile strength of concrete is $f_{cd} = 1.381$ MPa.

One end of the girder is modeled as a fixed hinge, restraining translations in x, y, and z directions and rotations about y and z. The opposite end is modeled as a movable support, restraining translations in x and y and rotations about y and z.

Mechanical properties of corrugated steel web box girders

Ultimate flexural capacity of positive bending sections

Due to the nonlinear stress–strain relationships of steel and concrete, the ultimate load-bearing capacity cannot be determined solely by strength limits. Material ductility and strain limits must also be considered. Therefore, elastic–plastic theory is adopted.

Assumptions

- Perfect composite action between steel web and concrete slabs.
- Tensile strength of concrete and flexural contribution of the steel web are neglected.
- Plane sections remain plane.
- Reinforcing steel follows a bilinear elastic–plastic law (Figure 5), and concrete follows a parabolic–rectangular law (Figure 6).

- The effective height of external tendons is constant.

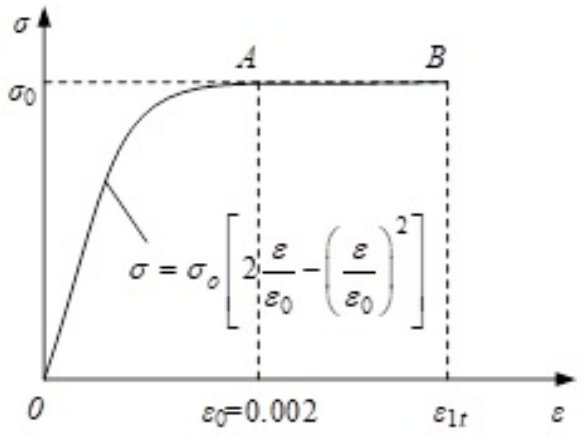

Figure 6: Constitutive relation of reinforcement

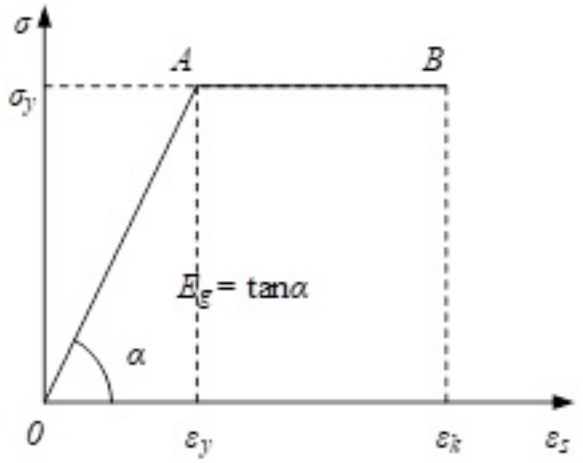

Figure 7: Constitutive relation of concrete

Strength formulation The equilibrium of axial forces gives

$$R_g A_g + R_y A_{y1} + \sigma_{yu} A_{y2} = R_a b_c x + R'_g A'_g + \sigma'_{yu} A'_y, \tag{1}$$

and the bending moment equilibrium yields the ultimate flexural capacity.

Shear buckling of corrugated steel webs

Three buckling modes are recognized: local buckling, global buckling, and interactive buckling. Sparse corrugations tend to local buckling, while dense corrugations favor global buckling.

Local buckling The critical shear stress for local buckling is

$$\tau_{cr,L} = \frac{\pi^2 E}{12(1-\mu^2)} \left(\frac{t}{b_w} \right)^2 k. \tag{2}$$

Global buckling The critical shear stress for global buckling is derived from energy methods and expressed as

$$\tau_{cr,G} = \frac{N_{cr}}{t}. \tag{3}$$

Combined buckling The interaction formula is

$$\frac{1}{\tau_{cr}} = \frac{1}{\tau_{cr,L}^4} + \frac{1}{\tau_{cr,G}^4}. \tag{4}$$

Shear strength verification

The allowable shear stresses for the three buckling modes are

$$[\tau_L] = \frac{\tau_{cr,L}}{\gamma_L}, \quad [\tau_G] = \frac{\tau_{cr,G}}{\gamma_G}, \quad [\tau_{cr}] = \frac{\tau_{cr}}{\gamma_{cr}}, \tag{5}$$

with safety factors $\gamma_L = 1.5$, $\gamma_G = 2.0$, and $\gamma_{cr} = 1.5$.

This comprehensive approach ensures that the corrugated steel web satisfies all relevant shear buckling and strength requirements under realistic bridge loading conditions.

STRUCTURAL AND MECHANICAL PERFORMANCE ANALYSIS OF CORRUGATED STEEL WEB BOX GIRDERS

Structural analysis of the corrugated steel web box girder

Overview of the case study

The selected case is a mega-span partially cable-stayed bridge located on the eastern side of the intersection of Century Avenue and Baizhang East Road. It represents a novel structural form within the new river-crossing bridge group of the eastern district and serves as a key transportation link between the old and new urban areas.

The superstructure consists of a three-span continuous variable-depth multi-cell box girder with a span arrangement of $30 + 55 + 30$ m. The total bridge width is 55 m, and the cross-section comprises five separated single-cell box girders. These girders are rigidly connected by a 0.5 m wide cast-in-place wet joint located at the center of the cantilevered wing slabs. The height of the outer edge girder at the abutment bearing section is 2.5 m, while the corresponding height at mid-span is 1.0 m. The bottom slab is horizontal, and the transverse slope of the deck is achieved through variations in web height. The lower edge of the box girder follows a circular arc profile.

Each side of the bridge includes 3×5 m long two-stage lap slabs. The bridge crosses the river orthogonally. A convex vertical curve with a radius of 1200 m is adopted at mid-span, and longitudinal slopes of 2.88% are

provided on both sides. The roadway has an outward cross slope of 2.2%, while the footway has an inward slope of 2.3%.

Within 15 m of each abutment, corrugated steel webs are employed, while the remaining regions with smaller beam heights use conventional concrete box girders. The bottom width of each single box girder is 6 m. The top width of both the central and side girders is 12 m, with a web thickness of 0.60 m and a top slab thickness of 0.40 m. The bottom slab thickness varies from 0.40 m at mid-span to 0.80 m at the pier. C50 concrete is adopted throughout. A 1.20 m thick transverse beam is installed at the pier, a 1.0 m thick diaphragm is provided at mid-span, and 0.40 m thick diaphragms are placed at both ends of the corrugated steel web segments.

Spatial finite element simulation

Due to the inherent randomness in vehicle trajectories, highway bridges are often subjected to eccentric loading. In practical design, this effect is typically addressed by introducing a load amplification factor. In this study, two loading scenarios are considered: symmetric loading (Case 1) and eccentric loading (Case 2), as defined previously. The ratio of the maximum structural response under Case 2 to that under Case 1 is defined as the vehicle load bias amplification factor, which serves as an indicator of the sensitivity of the corrugated steel web box girder to eccentric loading.

Taking the mid-span section as an example, the maximum positive bending moment M_1 under lane loading is first obtained from influence line analysis. According to the *General Specifications for Highway Bridges and Culverts*, lane loading is applied as a vertical load and does not account for transverse load distribution or eccentricity. To incorporate this effect, vehicle loading is used, which allows for asymmetric arrangements.

The vehicle loads are positioned along the influence line to obtain the maximum positive bending moment M_2 at mid-span. Ideally, M_2 should be equal to M_1. In practice, slight deviations occur. Based on the *Highway Bridge Load Test Code*, a ratio M_2/M_1 within the range of 0.85–1.05 is acceptable. In this study, $M_1 = 27{,}296$ kN·m and $M_2 = 27{,}234$ kN·m, giving $M_2/M_1 = 1.002$, which satisfies the requirement.

For Case 1, a total of seven standard vehicles are arranged symmetrically. Case 2 adopts the same longitudinal positions but introduces lateral eccentricity. Using the ANSYS spatial finite element model, the load amplification factors were computed for multiple sections. The results indicate that:

- The amplification factor for normal stress ranges from 1.02 to 1.20.
- The amplification factor for shear stress ranges from 1.10 to 1.51.

These results demonstrate that eccentric loading has a more pronounced effect on shear stress than on normal stress. Accordingly, it is recommended that a normal stress amplification factor of 1.15 and a shear stress amplification factor of 1.51 be adopted in practical bridge design to ensure adequate safety margins.

Mechanical performance evaluation of corrugated steel web box girders

Ultimate flexural capacity

An experimental investigation was conducted on two corrugated steel web box girders, denoted as Specimens A and B. Both specimens shared identical geometric and material properties. A comparison between the

calculated values obtained from the proposed theoretical formulas and the experimental results is summarized in Table 1.

Table 1: Comparison between theoretical predictions and experimental results

Specimen	Ratio	M_u (Exp.)	M_u (Calc.)	Ratio	T_u (Exp.)	T_u (Calc.)
A	0.5	64.8	62.6	1.03	176.13	196.22
B	1.0	156.4	199.6	0.78	164.72	162.23

The results indicate that the discrepancies between the predicted and measured ultimate capacities are within 15%. This level of accuracy satisfies engineering design requirements, confirming the applicability of the proposed formulation.

Shear buckling behavior

Local buckling The corrugated steel web was divided into 23 segments for analysis. The minimum local buckling strength was found to be 1359.24 MPa, which is significantly greater than the yield shear stress of 183.55 MPa. Hence, local buckling does not govern the design.

Global buckling The minimum critical stress associated with global buckling was 545.76 MPa, exceeding the yield shear stress of 169.24 MPa. This confirms that the global buckling resistance of the corrugated steel web is sufficient.

Interactive buckling The minimum combined buckling strength was 104.78 MPa, which remains lower than the combined critical shear stress of 149.42 MPa. This indicates that the interactive buckling mode also satisfies design requirements.

Shear strength verification

The shear strength of the corrugated steel web was further assessed using design code values. For Q345 steel, the design shear strength is 170 MPa for thicknesses up to 16 mm and 161 MPa for thicknesses between 16 mm and 35 mm. The finite element results show that the maximum shear stresses under ultimate limit state combinations remain below these thresholds, demonstrating full compliance with design specifications.

CONCLUSION

This study investigated the structural behavior and mechanical performance of corrugated steel web box girders in modern bridge applications using spatial finite element modeling.

1. Under symmetric loading (Case 1), the maximum positive bending moment at mid-span was 27,296 kN·m. Under eccentric loading (Case 2), the corresponding value was 27,234 kN·m, yielding a bias amplification factor of 1.002. Based on extensive numerical results, it is recommended to adopt amplification factors of 1.15 for normal stress and 1.51 for shear stress in practical design.

2. The discrepancy between calculated and experimental ultimate flexural capacities of the test girders was within 15%, satisfying the accuracy requirements of modern bridge engineering. Moreover, all shear buckling and shear strength verifications met code requirements, highlighting the excellent mechanical performance of corrugated steel web box girders.

REFERENCES

[1] Zhang Z, Zou P, Deng EF, Ye Z, Tang Y, Li FR. Experimental study on prefabricated composite box girder bridge with corrugated steel webs. Journal of Constructional Steel Research. 2023 Feb 1;201:107753.

[2] Li Q, Zhou M. Study on the natural frequency of box girders with corrugated steel webs. Journal of Constructional Steel Research. 2023 Dec 1;211:108123.

[3] Li L, Zhou C, Wang L. Distortion analysis of non-prismatic composite box girders with corrugated steel webs. Journal of Constructional Steel Research. 2018 Aug 1;147:74-86.

[4] Huang S, Cai C, Zou Y, He X, Zhou T, Zhu X. Experimental and numerical investigation on the temperature distribution of composite box-girders with corrugated steel webs. Structural Control and Health Monitoring. 2022 Dec;29(12):e3123.

[5] Zhang Z, Tang Y, Li J, Hai LT. Torsional behavior of box-girder with corrugated web and steel bottom flange. Journal of Constructional Steel Research. 2020 Apr 1;167:105855.

[6] Xu F, Cheng Y, Wang K, Zhou M. Transverse Analysis of Box Girders with Corrugated Steel Webs. Buildings. 2024 Feb 21;14(3):574.

[7] Zheng Y, Wang J, Guo P, Zhang Y. A Review of the Mechanical Properties of and Long-Term Behavior Research on Box Girder Bridges with Corrugated Steel Webs. Buildings. 2024 Sep 25;14(10):3056.

[8] Zhang F, Shen J, Liu J. Effect of encased concrete on section temperature gradient of corrugated steel web box girder. Advances in Structural Engineering. 2021 Aug;24(11):2321-35.

[9] Shi F, Wang D, Chen L. Study of flexural vibration of variable cross-section box-girder bridges with corrugated steel webs. InStructures 2021 Oct 1 (Vol. 33, pp. 1107-1118). Elsevier.

[10] Chen Y, Dong J, Xu T. Composite box girder with corrugated steel webs and trusses–A new type of bridge structure. Engineering Structures. 2018 Jul 1;166:354- 62.

[11] Zhang B, ChenW, Xu J. Mechanical behavior of prefabricated composite box girders with corrugated steel webs under static loads. Journal of Bridge Engineering. 2018 Oct 1;23(10):04018077.

[12] Kong X, Luo K, Ji W, Tang Q, Deng L. Study on dynamic characteristics of an improved composite box girder with corrugated steel webs. Journal of Bridge Engineering. 2022 Jun 1;27(6):04022035.

[13] He J, Liu Y, Wang S, Xin H, Chen H, Ma C. Experimental study on structural performance of prefabricated composite box girder with corrugated webs and steel tube slab. Journal of Bridge Engineering. 2019 Jun 1;24(6):04019047.

[14] Huang H, Zhang Y, Ji W, Luo K. Theoretical study and parametric analysis on restrained torsion of composite box girder bridge with corrugated steel webs. Journal of Bridge Engineering. 2022 Dec 1;27(12):04022118.

[15] Chen Y, Dong J, Xu T, Xiao Y, Jiang R, Nie X. The shear-lag effect of composite box girder bridges with corrugated steel webs and trusses. Engineering Structures. 2019 Feb 15;181:617-628.

[16] Qiao P, Di J, Qin FJ. Warping torsional and distortional stress of composited box girder with corrugated steel webs. Mathematical Problems in Engineering. 2018;2018(1):7613231.

[17] Li Y, Dai Q, Zhang Y, Liu C. Free vibration performance of curved composite box-girders with corrugated steel webs. Journal of Constructional Steel Research. 2021 Nov 1;186:106882.

[18] Mao YN, Ma C, Liu SZ, Li LY. Study on the dynamic response of composite box girder bridges with corrugated steel webs. Advances in Civil Engineering. 2023;2023(1):5104132.

[19] Ji W, Bai Q, Wang W, Li J. Fatigue study on improved composite box girder bridge with corrugated steel webs. Journal of Constructional Steel Research. 2024 Feb 1;213:108380.

[20] Zhang H, Chen Y, Pan J, Dong J, Zhao Q. Torsional behavior of super-span composite box girder with corrugated steel webs. InStructures 2024 Oct 1 (Vol. 68, p. 107045). Elsevier.

[21] Wang C, Zhang Y, Zhang X, Li Y,Wei X. Coupled bending-torsion behaviour of single-box multi-cell curved composite box-girders with corrugated-steel-webs. Journal of Constructional Steel Research. 2022 Sep 1;196:107411.

[22] Chen Y, Dong J, Tong Z, Jiang R, Yue Y. Flexural behavior of composite box girders with corrugated steel webs and trusses. Engineering Structures. 2020 Apr 15;209:110275.

[23] Cai C, Xu M, He X, Zou Y, Huang S. The thermal responses of composite box girder bridges with corrugated steel webs under solar radiation. Advances in Structural Engineering. 2024 Nov;27(15):2644-63.

[24] Tong Z, Shen K, Li Y, Dong J, Luo B. Modified Easley formula for elastic critical global shear buckling stress of corrugated steel webs considering real boundary conditions. Scientific Reports. 2024 Oct 21;14(1):24702.

[25] Zheng Y, Wang J, Guo P, Zhang Y. A Review of the Mechanical Properties of and Long-Term Behavior Research on Box Girder Bridges with Corrugated Steel Webs. Buildings. 2024 Sep 25;14(10):3056.

[26] Zhang H, Chen Y, Pan J, Dong J, Zhao Q. Torsional behavior of super-span composite box girder with corrugated steel webs. InStructures 2024 Oct 1 (Vol. 68, p. 107045). Elsevier. 71

B. w. Gong, School of Mechanical and Electronic Engineering, Hubei Polytechnic University, Huangshi, 435003, China

Abeer Abdullah Al Anazi, School of Mechanical and Electronic Engineering, Hubei Polytechnic University, Huangshi, 435003, China

Nader Ghareeb, College of Civil Engineering, Lanzhou Jiaotong University, Lanzhou, Gansu, 730070, China

Ahmad Sedaghat School of Mechanical and Electronic Engineering, Hubei Polytechnic University, Huangshi, 435003, China

Manuscript Published; 30 July 2024.